BeeNet: Reconstructing Flower Shapes from Electric Fields using Deep Learning

Jake Turley^{1, 2, 3}, Ryan A Palmer⁴, Isaac V Chenchiah², and Daniel Robert⁵

August 19, 2025

Abstract

Arthropods, including pollinators, respond to environmental electrical fields. Here, we show that electric field information can be decoded to reconstruct environmental features. We develop an algorithm capable of inferring the shapes of polarisable flowers from the electric field generated by a nearby charged bee. We simulated electric fields arising from bee–flower interactions for flowers with varying petal geometries. These simulated data were used to train a deep learning U-Net model to recreate petal shapes. The model accurately reconstructed diverse flower shapes including more complex flower shapes not included in training. Reconstruction performance peaked at an optimal bee–flower distance, indicating distance-dependent encoding of shape information. These findings show that electroreception can impart rich spatial detail, offering insights into arthropod environmental perception.

1 Introduction

Plants and arthropods have co-evolved over many millennia to form co-dependent relationships that vitally underpin the health of global ecosystems. These relationships are of the utmost importance to global food security since plants are a crucial food source and the reproduction of most plants requires arthropod-mediated pollination. The decline of pollinator populations, conjectured to be due to environmental and human stressors but whose causes remain unclear, invigorates the search for new understandings of the complex interactions between plants and arthropods.

Flower size, shape, colour, scent and temperature communicate information to pollinators that inform their decision making and underpin the sensitive ecological balance of the natural world. Such sensory cues have led to the evolution of multiple sensory perceptions and receptors in arthropods. From complex, sensitive receptors such as compound eyes and auditory systems, to general multifaceted sensors such as mechanosensory hairs, pollinator species have adapted in different ways to acquire and perceive these signals.

Recent research has shown that arthropods, including pollinators, respond to electrical fields arising, for example, from flowers and atmospheric potentials. This sensory capacity of living organisms to detect electric fields is known as electroreception. Though this electric sensitivity has been studied

¹School of Biochemistry, University of Bristol, Biomedical Sciences Building, University Walk, Bristol BS8 1TD, UK

 ²School of Mathematics, University of Bristol, Fry Building, Woodland Road, Bristol, BS8 1UG, UK
 ³Mechanobiology Institute, National University of Singapore, 5A Engineering Drive 1, Singapore 117411
 ⁴School of Engineering Mathematics and Technology, University of Bristol, Ada Lovelace Building, University Walk, Bristol, BS8 1TW, UK

⁵School of Biological Sciences, University of Bristol, Life Sciences Building, 24 Tyndall Avenue, Bristol, BS8 1TQ, UK

in aquatic and, more recently, aerial environments [1, 6, 7, 10, 11, 17, 30, 34, 45], its implications remain largely unexplored, prompting questions about electrical ecology and interactions [13,24,25,26,27,28].

Many studies have focused on the electrical sensory abilities of arthropods and some of the remarkable behavioural implications in communication [17], foraging [1,30], dispersal [34], parasitism [10] and pollination [6]. Such behavioural and mechanical evidence motivates investigation of floral electrics as part of the rich ecology of plants and arthropods. Indeed, a growing number of papers have considered the electrostatics of plants [25, 32, 33, 35, 38]. Yet, further research into the information contained in floral electric fields is required to ascertain how a flower may produce ecologically-relevant electrical signals that are detectable by arthropods. Thus, in this paper we investigate what information about a flower's morphology and material properties can be deduced from its electric field.

The investigation herein complements our earlier work on the mechanics of electroreceptive hair sensing and implications for biology [12, 39, 40, 41, 42, 43]. In particular, it furthers the work began in [42], which demonstrated that the location and shape of a (non-polarisable) electrical object can be deduced from the deflections of an arthropod's electroreceptive hairs. Here, we turn our attention to the mathematically more subtle case of polarisable objects, of which flowers are an example.

Moreover, since our focus is on the information contained in electric fields, and not on the sensory mechanisms, we turn our attention from the deflections of electroreceptive hairs in an electric field to the electric fields themselves. Thus, instead of detailed computations involving hair deflections we use AI tools to uncover information relating to proximity and geometry contained in electrical fields. In addition to introducing AI tools to this area of mathematical biology, this also entails that our results are sensor agnostic.

AI tools are increasingly applied to help study biological systems, e.g. [9, 19, 47]. In particular, deep learning models have long been used to identify and segment objects such as nuclei, and cells in images [2, 44, 47, 51, 52]. They have also been used to detect and classify dynamic cell behaviours such as cell divisions and extrusions [31, 50, 52, 53]. Here, we extend these tools to electroreception by developing an AI model ("BeeNet") which can reconstruct the shapes of flowers without directly observing them but using instead information about the electrical fields produced from the interaction between flowers and charged arthropods.

2 Methods

Modelling electrical fields 2.1

Floral electrical fields. We consider a scenario in which a positively-charged bee [6,7] approaches an uncharged, polarisable flower. The flower responds by polarising, i.e. it develops an opposing electrical field, whose structure and strength depends on the shape and material properties of the flower. To model this scenario, the flower is treated as a two-dimensional dielectric whose boundary is described through an analytic function.

Labelling the interior, exterior and boundary of the flower as Ω_1 , Ω_2 and Γ , respectively, the electrical field E can be written as the gradient of the electric potential,

$$V = \begin{cases} V_1 & \text{in } \Omega_1, \\ V_2 & \text{in } \Omega_2, \end{cases} \tag{1a}$$

which satisfies

$$E = -\nabla V, \tag{1b}$$

$$\Delta V_1 = 0 \qquad \text{in } \Omega_1, \tag{1c}$$

$$\Delta V_1 = 0$$
 in Ω_1 , (1c)
 $\Delta V_2 = 0$ in Ω_2 , (1d)

$$V_1 = V_2 \quad \text{on } \Gamma, \tag{1e}$$

$$\frac{\partial V_2}{\partial n} = \tilde{\epsilon} \frac{\partial V_1}{\partial n} \text{ on } \Gamma, \tag{1f}$$

where $\tilde{\epsilon} = \epsilon_1/\epsilon_2$ is the ratio of the absolute permittivities of the flower and the surrounding air.

Boundary conditions (1e) and (1f) are a consequence of the electrical potential's continuity across the boundary and of Gauss' Law, respectively [18]. The far-field condition on the potential V_2 depends upon how E is generated.

Arthropod electrical fields. Next, consider an arthropod, say a bee, with a charge λ centred at the point $z_B^* = Lz_b$ which is typically several 'petal radii', L, away from $z^* = Lz$ (i.e. a similar order of magnitude to the flower size). We assume that the arthropod is sufficiently small and, therefore, considering it as a point charge, its electric potential in two-dimensional free space is,

$$V^* = -\frac{\lambda}{2\pi\epsilon} \log|z^* - z_B^*| = -Q\log|z^* - z_1^*|, \tag{2}$$

where the absolute permittivity ϵ is ϵ_1 in Ω_1 and ϵ_2 in z_2 . The potential V is scaled by Q as $V^* = QV$, where V^* is non-dimensional quantity we compute in our datasets. The far-field condition is

$$V_2 \to -\log|z - z_1| - \log|L|$$
 as $|z| \to \infty$, (3)

as detailed in [21].

Solving for the electric fields. The recently-developed two-domain AAA-least squares (2D-2D-AAA-LS) method [21] is used to solve the system of equations above. This method solves for the harmonic electric potential V both inside and outside of a flower, subject to prescribed conditions at the flower-air interface and for prescribed far-field behaviour. It is an extension of the AAA-LS method, which has become popular over the last few years with application to problems in mathematics, physics, chemistry and biology [20, 29, 37, 55] and has been extended [16, 37] to incorporate multiply connected domains [8, 49] and other governing equations such as the Stokes [3], Poisson [20] and Helmholtz [15] equations.

Full details of the solution method are given in [21]. In brief, solving the above equations, the potential V is given as the real part of some analytic function F(z) that is approximated by rational functions, i.e. a polynomial plus the sum of singular terms from poles positioned near the corners and cusps of the flower boundary. The function F is then found using a linear least squares (LS) algorithm.

Whilst other methods, such as finite element methods, can be used to solve the above problem, the 2D-AAA-LS algorithm is mesh-free, fast, and accurate: First, the 2D-AAA-LS algorithm provides an analytic solution based solely on the far-field conditions, the floral boundary and the interfacial conditions. Since the boundary is given by an analytic function, it can be quickly and efficiently changed via a simple adaptation of the generating parameters in an unsupervised manner. Mesh-based methods would require meshing for each geometry, requiring more time and less automation. Second, the method is fast, typically solving each case in a fraction of a second. The speed of this method enables vast numbers of scenarios to be investigated efficiently, lending itself to machine learning/AI approaches. Third, the result is highly accurate, producing relative errors in the order of 10^{-16} to 10^{-6} compared to analytical solutions and in contrast to relative errors of 10^{-2} in FEM approaches [21].

2.2 Generating the data set

Using the above method, we investigate the reconstruction of floral shapes via electrical fields by considering several different scenarios and shapes that illustrate possible pollinator-plant interactions found in nature. Our topic of interest is how an uncharged dielectric flower polarises in the presence of some external electrical field, altering the field and what information about the flower's shape and location this field may provide to an arthropod at a distance.

To measure how the flower perturbs the source field we use the 'perturbation field' of the flower,

$$V_P = V - V_B, (4)$$

$$||E_P|| = ||E - E_B||, (5)$$

where the subscript P indicates a perturbation value, B indicates a scenario where only the charged arthropod is present, and the terms without subscripts are those of the modelled scenario, i.e. flower and bee.

From a sensory biology perspective, it is natural to assume that the source (i.e. bee) does not detect itself and thus its contribution to the electric field can be subtracted. It is also computationally natural since the bee's electrical field dominates the flower's polarised field close to the bee's location. Thus, the perturbation field may be interpreted as the 'floral electrical information' from an arthropod's perspective and enables us to assess and compare changes in the field strength and structure as the flower distorts the source electrical field.

Data generation was automated in MATLAB 2023b. Overall, 1,979 datasets were produced, in which the floral shape, number of petals, flower orientation, floral permittivity and distance of the arthropod to the flower were varied, as shown in Figure 1. In each scenario, the 2D-AAA-LS algorithm was used to produce the electrical potential and electrical fields solutions. After which, the solution were evaluated on a 801-by-801 square mesh to obtain the perturbation potential, V_P and the perturbation electrical field $E_P = (E_{P,x}, E_{P,y})$.

The fields were normalised to lie in [0,1] which is a typical input range for images in deep learning algorithms. We establish a maximum absolute value for the potential field (V_{max}) such that it trims only the highest values within the images (typically at the petal tips) while preserving high contrast across the majority of the field. This is needed as the inclusion of extreme values in the normalisation process can obscure much of the signal in the remainder of the image. After trimming the highest absolute values we apply this normalisation:

$$\tilde{V_P} = 0.5 + \frac{V_P}{2V_{max}} \tag{6}$$

with similar normalisation for $E_{P,x}$ and $E_{P,y}$.

The fields can then be represented as a greyscale image, wherein negative values appear as dark regions, positive values as lighter regions (Figure 1B). The three greyscale images are reduced in size to 401x401 pixels which still maintains a high resolution of the electric fields but reduces the memory and computational power required for model training. After size reduction, the images are combined into a single 16-bit RGB image as in Figure 1C. These RGB images contain all the computed information about the flower's electric field in a format suitable for computer vision deep learning algorithms.

Since the shape of the petal is clearly visible in the field (Figure 1B), we hid this information as follows: Every flower is constrained to lie in a disk of radius L, and a disk of radius of 1.1L is excluded from each dataset. This ensures that only information about the surrounding electric fields produced from the flower-bee interaction is retained. This is interpreted as the electrical sensory information that is propagated by the flower.

Finally, each of these input images is matched with a binary petals mask, outlining the floral geometry (Figure 1C). Our goal is to train deep learning algorithms to reproduce these petal masks from the images containing information about the electrical fields (Figure 1D).

2.3 U-Net models for reconstructing flower shapes from electrical fields

To reconstruct flowers from their electric fields, we use a deep learning segmentation algorithm based on the U-Net architecture, a widely used and highly effective model [46]. Unlike traditional segmentation, which identifies objects with clearly defined visual boundaries, this task involves inferring shape from electric field features at a distance, making it more complex. Nevertheless, we show that the same model architecture can be applied successfully. To make a model to complete this task, we converted an image classifier model ResNet101 into a U-Net structure via the fast ai library's Dynamic U-Net class function [22,23]. A sketch of a simplified architecture of the model is displayed in Figure 1D and the model output with its ground truth mask (labelled data) is shown in Figure 1E.

Training deep learning models typically requires a large volume of data [?, 19]. Therefore, we produced a large variety of floral examples as noted above and shown in Figure 1F. The model is

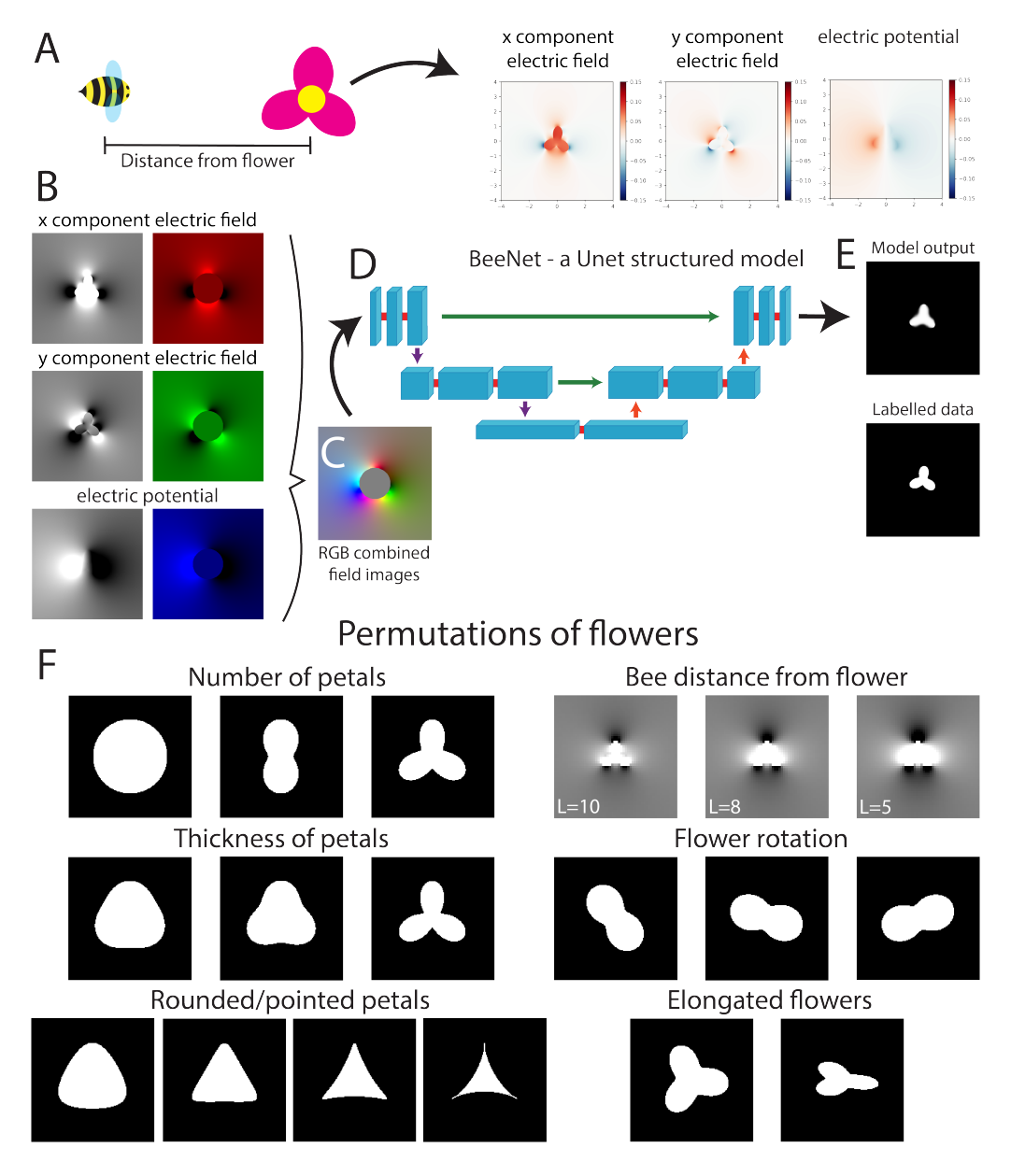


Figure 1: A) Diagram of bee and flower with the change in electric fields as result of the flower. B) The 3 fields converted to images. C) Combined images to form a single RGB image. D) A simplified sketch of the BeeNet model. E) The output of the model with the labelled data. F) The different permutations of the flowers used in training.

trained solely on flowers with one to three rounded petals. Since the bee is the source of the electric field in which the flower polarises, the distance between the bee and the flower affects the floral field and its strength. This parameter is varied to generate test data ranging from five to ten petal radii from the flower. Lastly, we produced all of the above data for two values of relative floral permittivity, $\tilde{\epsilon}$ (see (1f)), 10 and 20; this affects the strength of the perturbed electric field. Consequently, with all these perturbations a large training dataset was produced.

To determine the model's effectiveness, we tested it on four-petal flowers to see if it could reconstruct these despite having never encountered them previously. Furthermore, we also varied the petal thickness and shape (e.g. pointed or rounded), rotated the flowers relative to the bee, stretched the flowers, and even removed petals to test whether the model could reconstruct the floral geometries in a range of scenarios and cases it had not been previously exposed to (Figure 1F).

Datasets. The data were divided into three sets:

First, the training set comprised flowers with one to three petals, with all possible permutations depicted in Figure 1F. Every rotation of the flower relative to the bee was employed except one, which was reserved for the subsequent set.

Second, the validation set contains the same permutations as the training set but at a single, distinct rotation with respect to the bee. Essentially, it includes identical flower shapes as the training set but in unfamiliar rotations.

Third, the test set consists exclusively of four-petal flowers. This will evaluate the model's ability to identify flowers, even though it has not been trained to recognize these specific shapes.

The data were augmented using the albumentations library [4]. The transforms used were Rotate, HorizontalFlip and VerticalFlip.

Network architecture and training models. We converted a Resnet101 model into a U-Net architecture via the Dynamic UNET function from the fast ilibrary [22, 23, 46, 50, 52]. The weights from the Resnet101 classifier were used to take advantage of transfer learning [?]. BeeNet has 318,616,725 parameters and has 121 layers. This model has inputs of 401 x 401 x 3. Source code is available at https://github.com/turleyjm/BeeNet and training data can be downloaded from https://zenodo.org/records/16879470.

Paperspace's gradient ML Platform was used for training the models. The machine used was one with NVIDIA Quadra P5000 or P6000 GPU. We trained using an Adam optimization. [36].

3 BeeNet can learn to infer flower structure based on the electric field.

We initially evaluated the model using the validation data set, which includes the identical flower shapes found in the training data set but presented at a different unseen orientation relative to the bee. Subsequently, we tested the model on a dataset with four petal types that it had not previously encountered.

3.1 The model's reconstruction of familiar flower shapes

To demonstrate the effectiveness of the model in reconstructing flowers we overlay the output (magenta) and the ground truth mask (green) as shown in Fig. 1A. The white regions are correctly identified areas of flower petals; these are the true positives, T_p . Green displays false negative areas, F_n , where the petals should be, but have not been captured by the model. The magenta regions are false positives, F_p , which the model has incorrectly determined as parts of flowers. To quantify the effectiveness of

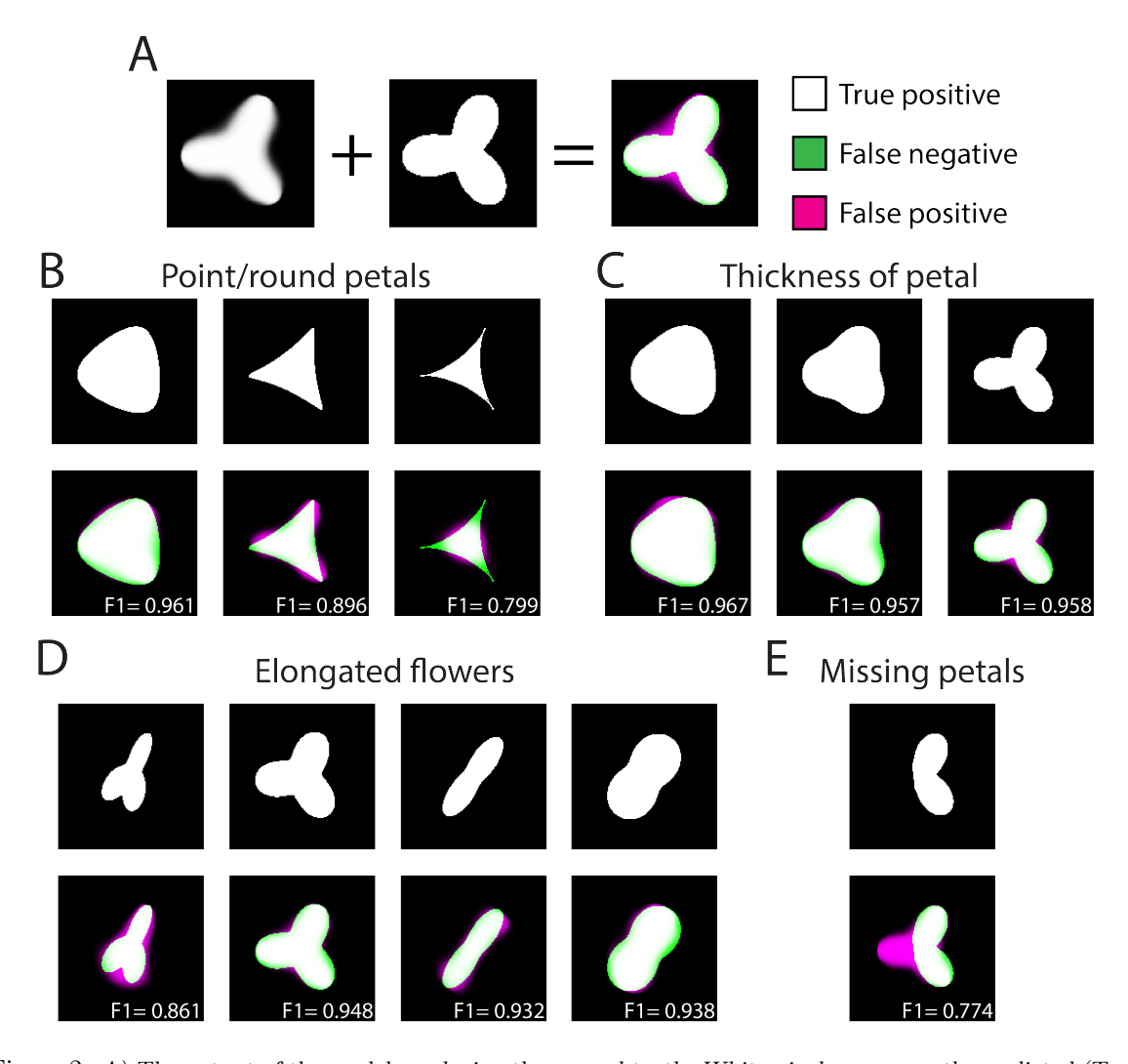


Figure 2: A) The output of the model overlaying the ground truth. White pixels are correctly predicted (True positive). Green and magenta are the false negatives and false positives, respectively. B-E) The ground truth with the overlapping images displaying the accuracy for each of the shape perturbations

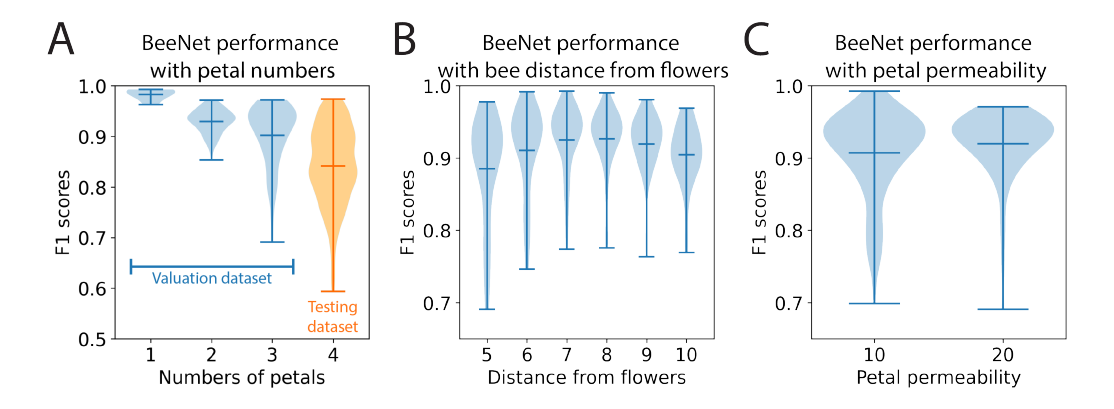


Figure 3: A) Violin plot of the F1 score for each number of petals in flowers. The valuation dataset was used for flowers with 1-3 petals (blue) and test set was used for 4 petal flowers (orange). B) The F1 score performs with the bees distance from a flower. The valuation dataset was used

the model we will use a standard metric F1 score [?]:

$$F1 = \frac{2T_p}{2T_p + F_p + F_n}. (7)$$

A perfect F1 score of 1 indicates the image has been flawlessly reconstructed. Smaller values of F1 indicate decreased accuracy.

The validation data set featured the same floral shapes as the training dataset, however these were rotated relative to the bee, providing a previously 'unseen' configuration. The model was trained on these shapes but not seen them at this rotation relative to the position of the bee. On average, across all shapes in the validation set, we obtained an F1 score of 0.912. Comparing different petal counts in flowers, we found that the model reconstructed circular shapes most accurately, achieving an average F1 score of 0.983 (Fig. 3A). For flowers with two and three petals, the scores dropped to 0.929 and 0.902, respectively. This indicates that as floral complexity increases, the model's ability to reconstruct geometry from its electrical field at a distance decreases, though overall F1 scores remain high.

We examined whether altering the petals' permeability could modify the electric field and enhance the model's informational intake. In the validation dataset, raising the relative permeability of the petals from 10 to 20 led to a modest improvement in performance, increasing the average F1 score from 0.907 to 0.920 (Fig. 3C). This boost largely stems from better performance in the flowers with the worst initial reconstructions. When the relative permeability was 10, there were numerous flowers with scores ranging from 0.75 to 0.85, but at a relative permeability of 20, the performance of these flowers substantially improved (Fig. 3C). This result is unsurprising, as higher permittivity amplifies the strength of the electric field, thereby more accurately reflecting the floral geometry.

Since the flower polarises in the presence of the bee, the distance between the two influences the strength of the electrical field and thus the quality of the information used by the model to reproduce the flowers structure. Based on this physical law we expected that a closer bee, producing a stronger floral electrical fields, would lead to more information for the reconstruction. After measuring the average F1 score from our database of petals we found that there was a modest increase in the accuracy in the middle of our range peaking at 8 petal radii from the flower with a score of 0.927 shown in Fig. 3B. While at 5 and 10 petal radii mean values were 0.885 and 0.904, respectively. This result suggests that there is an optimum distance from the flower in which its electric field can be used to determine its shape.

We also investigated the role the petal shape to determine how changes in the floral geometry affect the reconstruction, e.g. pointed versus rounded petals or different petal thicknesses. Flowers with rounded petals are closer to the circular geometry which we have previously shown to possess

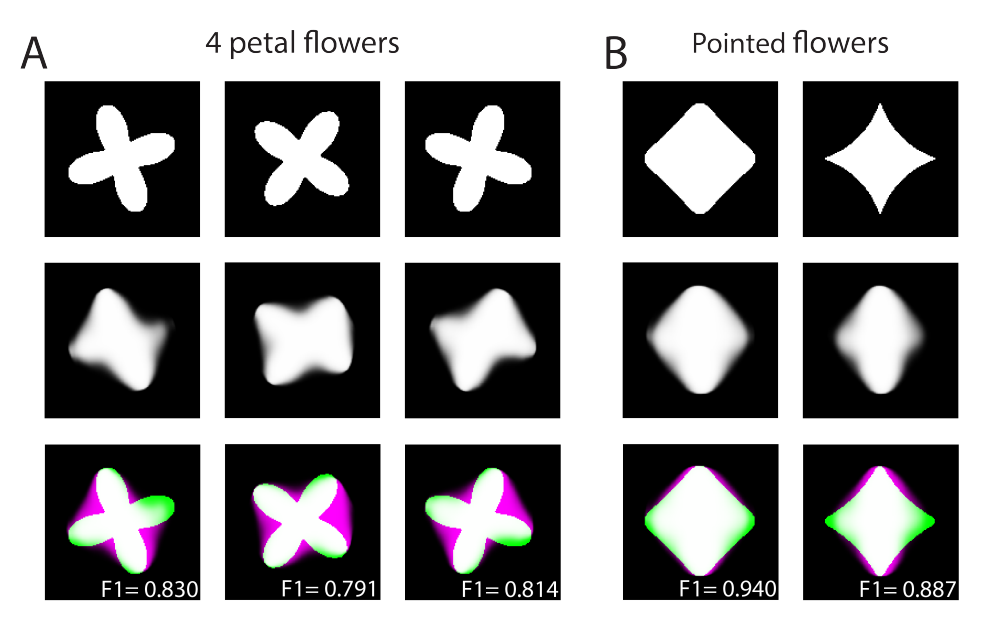


Figure 4: A) Overlapping images displaying the accuracy for different rotations of the 4 petal flowers. B) 4 petal flowers with different levels of pointedness. (Green and magenta are the false negatives and false positives, respectively.)

a high accuracy in their reconstruction. Such petals had a high mean F1 score of 0.944 whereas the model struggled to segment pointed petals with an average score of 0.785. The largest inaccuracies occurred around the petal tips which the model failed to recognise (Fig. 2B). Thicker petals led to a small increase in accuracy (Fig. 2C), whilst petal elongation led to a small decrease in accuracy as mainly seen in three-petal flowers where there was a decrease in F1 score from 0.914 to 0.876 (Fig. 2D). Lastly, when we removed a petal from the three petal flowers the model incorrectly 're-added' the petal into the shape, giving it a low F1 score (Fig. 2E).

3.2 BeeNet can reconstruct novel floral structures, albeit with reduced refinement.

We evaluated the model's ability to reconstruct previously unseen flower shapes, testing its capacity to classify novel flower shapes rather than relying solely on learned geometries. For this assessment, we selected four-petal flowers (Fig. 4).

Fig. 4A shows that while the general four-petal structure is preserved, the reconstructions are less clear and sharp than those of previously seen flowers. The average F1 score for four-petal flowers is 0.842, lower than 0.902 for three-petal flowers (Fig. 3A), which aligns with the trend of decreasing accuracy for more complex and unfamiliar shapes.

Petals along the vertical axis are reconstructed more accurately than those along the horizontal axis, where some are missing or nearly lost. This suggests that electrical field information—along the y-axis plays a greater role in reconstruction accuracy: Since the bee is positioned to the left of each flower, vertical components, which are perpendicular to the floral shape, provide more distinctive information than parallel components. Despite these challenges, the model can segment various four-petal flower shapes, capturing their overall structure with reasonable accuracy (Fig. 4B).

4 Discussion

In this study we have developed a deep learning model called BeeNet which can reconstruct the shapes of flowers solely from their electrical field. BeeNet is shown to successfully segment shapes using the mid- to long-range strength and shape of the floral electric fields with a high level of precision.

In contrast to this focus on electrostatic floral signals, hitherto the majority of modelling has focussed on the mechanics of hairs sensors, as opposed to the nature of the signals they receive. Indeed, this current paper is a complement to recent work that studied object reconstruction via the electromechanical actuation of sensory hairs [42]. Therein, the possibility that the strength, structure and shape of a generating object could be reconstructed by an observer was examined solely through the deflection of sensory hairs. However, within this current paper, the research question differs in two ways:

First, a 'sensor' agnostic approach is followed. That is, whilst the field strength and potential are known, how this information is obtained is not considered. Therefore, our work investigates the problem of object reconstruction from an information-theoretic point view, i.e. what in the nature of electrical fields produces information that is potentially acquirable, interpretable and usable by an observer. Second, the information considered herein is that of the electrical field about a flower due to polarisation caused by a static observer at a single location. Conversely, in [42], several observations are made by an observer of a statically charged object with no polarisation. Hence, the electrical information used to reconstruct the objects is physically different in both instances.

Returning to the role of floral geometry in electrostatic signals, crucially, BeeNet accurately distinguishes between different thicknesses, shapes and numbers of the petals based solely on the electrical field's variation and magnitude. This reveals the potential utility and nature of electrostatic sensory information within the wider sensory ecology of arthropods. Throughout the analysis, we show that flowers produce distinct electrical 'signatures' within the electrical field, enabling the flower's shape, orientation and distance to be predicted by an electrosensitive observer.

Our analyses also shows how the shape, orientation and distance of the flower lead to strong qualitative and quantitative changes in predictability of the electrical field shape and strength. Thus, our results indicate that the broad variation of flower morphology [5] can lead to distinct detectable and differentiable signals that convey perceptibly unique information about the flower [21].

In addition to being reconstructing flowers previously seen and learned by the model we pushed this one step further testing unseen types of flowers. While the quality of the segmentation was reduced, the approximate shapes of the flowers is visible in these outputs. This demonstrates that the model is able to fundamentally gather information about flower shapes from electric fields rather than simply remembering (over fitting) shapes it has previously learned from. This indicates further utility of this sense in, e.g. determining plant health.

4.1 Future Work

Since this is a two-dimensional study, several aspects of flower morphology and heterogeneity such as three-dimensionality and plant sex organs [5], are not captured by our analysis. We anticipate such features would further enhance the reconstruction of different floral shapes in three dimensions.

In our study we also found that there is potentially an optimal distance between the bee and flower at which the polarised floral fields best conveys information for reconstruction and identification. This relationship should be further studied including whether there is also dependency on the strength of the electric field in finding the best distance for flower identification.

A dynamic equivalent of the model is also worth exploring. That is, to study the variation in electric field as a bee moves around a flower and the possibility of identifying flowers from this variation.

4.2 Conclusions

As discussed in [41], the strength, direction and influence of the electrical modality has distinct underlying physics compared to other senses. Electrostatics therefore present a particularly novel modality in the sensory world of arthropods since few other modalities, other than vision, can elicit non-contact geometrical information, at a distance, for decision making. Thus, electrical fields present the possibility of a unique, information rich and distinguishable channel of information that is pervasive throughout each natural environment.

Emperical and modelling studies are beginning to provide more evidence of the nuances of electrical field sensing in arthropods and this modality's wider role in arthropod sensory ecology [7, 13, 14, 30, 34, 48]. Taking the results of this present study in the context of these experimental studies and other recent work on floral electrostatics [21,54] and object reconstruction via sensory hairs [42], the potential power of electroreception and the information that can be conveyed and acquired is becoming clearer and more compelling. This is true both from the side of electromechanical sensors and arthropod neurology, as well as the underlying physics that underpin the shape, strength and signal produced by electrical fields in nature.

References

- [1] AMADOR, G. J., MATHERNE, M., WALLER, D., MATHEWS, M., GORB, S. N., AND HU, D. L. Honey bee hairs and pollenkitt are essential for pollen capture and removal. *Bioinspir. Biomim.* 12, 2 (2017), 026015.
- [2] BARONE, V., TAGUA, A., ROMÁN, J. A. A.-S., HAMDOUN, A., GARRIDO-GARCÍA, J., LYONS, D. C., AND ESCUDERO, L. M. Local and global changes in cell density induce reorganisation of 3D packing in a proliferating epithelium. *Development 151*, 20 (05 2024), dev202362.
- [3] BRUBECK, P. D., AND TREFETHEN, L. N. Lightning Stokes solver. SIAM J. Sci. Comput. 44, 3 (2022), A1205–A1226.
- [4] Buslaev, A., Iglovikov, V. I., Khvedchenya, E., Parinov, A., Druzhinin, M., and Kalinin, A. A. Albumentations: Fast and flexible image augmentations. *Information (Switzerland)* 11, 2 (Feb. 2020). arXiv: 1809.06839 Publisher: MDPI AG.
- [5] BYNG, J. W., SMETS, E. F., VAN VUGT, R., BIDAULT, E., DAVIDSON, C., KENICER, G., CHASE, M. W., AND CHRISTENHUSZ, M. J. The phylogeny of angiosperms poster: a visual summary of APG IV family relationships and floral diversity. *The Global Flora* 4, 7 (2018), 1–4.
- [6] CLARKE, D., MORLEY, E., AND ROBERT, D. The bee, the flower, and the electric field: electric ecology and aerial electroreception. *J. Comp. Physiol. A* 203, 9 (2017), 737–748.
- [7] CLARKE, D., WHITNEY, H., SUTTON, G., AND ROBERT, D. Detection and learning of floral electric fields by bumblebees. *Science* 340, 6128 (2013), 66–69.
- [8] Costa, S., and Trefethen, L. N. AAA-least squares rational approximation and solution of Laplace problems. In *Euro. Congress Math.* (2023), pp. 511–534.
- [9] CULLEY, S., CABALLERO, A. C., BURDEN, J. J., AND UHLMANN, V. Made to measure: An introduction to quantifying microscopy data in the life sciences. *Journal of Microscopy* (2023). Publisher: John Wiley and Sons Inc.
- [10] England, S. J., Lihou, K., and Robert, D. Static electricity passively attracts ticks onto hosts. *Curr. Bio.* (2023).

- [11] ENGLAND, S. J., PALMER, R. A., O'REILLY, L. J., CHENCHIAH, I. V., AND ROBERT, D. Electroreception in treehoppers: How extreme morphologies can increase electrical sensitivity. *Proceedings of the National Academy of Sciences* 122, 30 (2025), e2505253122.
- [12] ENGLAND, S. J., PALMER, R. A., O'REILLY, L. J., CHENCHIAH, I. V., AND ROBERT, D. Electroreception in treehoppers: How extreme morphologies can increase electrical sensitivity. *Proceedings of the National Academy of Sciences* 122, 30 (2025), e2505253122.
- [13] ENGLAND, S. J., AND ROBERT, D. The ecology of electricity and electroreception. *Bio. Rev.* 97 (2021), 383–413.
- [14] ENGLAND, S. J., AND ROBERT, D. Prey can detect predators via electroreception in air. *Proceedings of the National Academy of Sciences* 121, 23 (2024), e2322674121.
- [15] GOPAL, A., AND TREFETHEN, L. N. New Laplace and Helmholtz solvers. PNAS 116, 21 (2019), 10223–10225.
- [16] GOPAL, A., AND TREFETHEN, L. N. Solving Laplace problems with corner singularities via rational functions. SIAM J. Num. Anal. 57, 5 (2019b), 2074–2094.
- [17] GREGGERS, U., KOCH, G., SCHMIDT, V., DÜRR, A., FLORIOU-SERVOU, A., PIEPENBROCK, D., GÖPFERT, M. C., AND MENZEL, R. Reception and learning of electric fields in bees. Proc. Roy. Soc. B 280, 1759 (2013), 20130528.
- [18] Griffiths, D. J. Introduction to electrodynamics, 2005.
- [19] HALLOU, A., YEVICK, H. G., DUMITRASCU, B., AND UHLMANN, V. Deep learning for bioimage analysis in developmental biology. *Development (Cambridge)* 148, 18 (Sept. 2021). Publisher: Company of Biologists Ltd.
- [20] Harris, S. J., and McDonald, N. R. Penguin huddling: a continuum model. *Acta Appl. Math.* 185, 1 (2023), 7.
- [21] HARRIS, S. J., PALMER, R. A., AND MCDONALD, N. R. Modeling floral and arthropod electrostatics using a two-domain aaa-least squares algorithm. SIAM Journal on Applied Mathematics 85, 2 (2025), 916–944.
- [22] HE, K., ZHANG, X., REN, S., AND SUN, J. Deep Residual Learning for Image Recognition. *IEEE Xplore* (2016).
- [23] Howard, J., and others. Fast.ai, 2018.
- [24] Hunting, E. R. Atmospheric electricity: an underappreciated meteorological element governing biology and human well-being. *Int. J. Biometeorol.* 65, 1 (2021), 1–3.
- [25] HUNTING, E. R., ENGLAND, S. J., KOH, K., LAWSON, D. A., BRUN, N. R., AND ROBERT, D. Synthetic fertilizers alter floral biophysical cues and bumblebee foraging behavior. *PNAS Nexus* 1, 5 (2022), 1–6.
- [26] HUNTING, E. R., ENGLAND, S. J., AND ROBERT, D. Tree canopies influence ground level atmospheric electrical and biogeochemical variability. *Front. Earth Sci. 9* (2021), 671870.
- [27] Hunting, E. R., Matthews, J., de Arróyabe Hernáez, P. F., England, S. J., Kourtidis, K., Koh, K., Nicoll, K., Harrison, R. G., Manser, K., Price, C., et al. Challenges in coupling atmospheric electricity with biological systems. *Int. J. Biometeorol.* 65 (2021), 45–58.

- [28] HUNTING, E. R., O'REILLY, L. J., HARRISON, R. G., MANSER, K., ENGLAND, S. J., HARRIS, B. H., AND ROBERT, D. Observed electric charge of insect swarms and their contribution to atmospheric electricity. iScience 25, 11 (2022), 105241.
- [29] Kehry, M., Klopper, W., and Holzer, C. Robust relativistic many-body Green's function based approaches for assessing core ionized and excited states. *J. Chem. Phys.* 159, 4 (2023).
- [30] KHAN, S. A., KHAN, K. A., KUBIK, S., AHMAD, S., GHRAMH, H. A., AHMAD, A., SKALICKY, M., NAVEED, Z., MALIK, S., KHALOFAH, A., ET AL. Electric field detection as floral cue in hoverfly pollination. Sci. Rep. 11, 1 (2021), 1–9.
- [31] McDole, K., Guignard, L., Amat, F., Berger, A., Malandain, G., Royer, L. A., Turaga, S. C., Branson, K., and Keller, P. J. In Toto Imaging and Reconstruction of Post-Implantation Mouse Development at the Single-Cell Level. *Cell* 175, 3 (Oct. 2018), 859– 876.e33. Publisher: Cell Press.
- [32] MOLINA-MONTENEGRO, M. A., ACUÑA-RODRÍGUEZ, I. S., BALLESTEROS, G. I., BALDELO-MAR, M., TORRES-DÍAZ, C., BROITMAN, B. R., AND VÁZQUEZ, D. P. Electromagnetic fields disrupt the pollination service by honeybees. *Sci. Adv. 9*, 19 (2023), eadh1455.
- [33] Montgomery, C., Vuts, J., Woodcock, C. M., Withall, D. M., Birkett, M. A., Pickett, J. A., and Robert, D. Bumblebee electric charge stimulates floral volatile emissions in petunia integrifolia but not in antirrhinum majus. *Sci. Nat.* 108 (2021), 1–12.
- [34] Morley, E. L., and Robert, D. Electric fields elicit ballooning in spiders. Curr. Bio. 28, 14 (2018), 2324–2330.
- [35] MOYROUD, E., AND GLOVER, B. J. The physics of pollinator attraction. New Phytol. 216, 2 (2017), 350–354.
- [36] Najafi Salehi, J., Eimani, H., Shahverdi, A., Totonchi, M., Fathi, R., Moosavi, S. A., Taher Mofrad, S. M. J., and Tahaei, L. S. Improvement of mouse preantral follicle survival and development following co-culture with ovarian parenchyma cell suspension. *International Journal of Fertility and Sterility* 18, 2 (2024), 153–161.
- [37] NAKATSUKASA, Y., SETE, O., AND TREFETHEN, L. N. The first five years of the AAA algorithm. arXiv preprint arXiv:231203565 (2023).
- [38] Nanda, I., De, R., et al. Study of electromagnetic radiation on flower. *Matrix Sci. Math.* 6, 2 (2022), 58–63.
- [39] Palmer, R. A., Chenchiah, I. V., and Robert, D. Analysis of aerodynamic and electrostatic sensing in mechanoreceptor arthropod hairs. *Journal of Theoretical Biology* 530 (Dec. 2021). Publisher: Academic Press.
- [40] Palmer, R. A., Chenchiah, I. V., and Robert, D. The mechanics and interactions of electrically sensitive mechanoreceptive hair arrays of arthropods. *Journal of the Royal Society Interface* 19, 188 (2022). Publisher: Royal Society Publishing.
- [41] PALMER, R. A., CHENCHIAH, I. V., AND ROBERT, D. Passive electrolocation in terrestrial arthropods: Theoretical modelling of location detection. *Journal of Theoretical Biology* 558 (Feb. 2023). Publisher: Academic Press.
- [42] Palmer, R. A., Chenchiah, I. V., and Robert, D. Sensing electrical environments: mechanical object reconstruction via electrosensors. *Journal of Physics A: Mathematical and Theoretical* 57, 38 (sep 2024), 385601.

- [43] Palmer, R. A., O'Reilly, L. J., Carpenter, J., Chenchiah, I. V., and Robert, D. An analysis of time-varying dynamics in electrically sensitive arthropod hairs to understand real-world electrical sensing. *Journal of the Royal Society Interface 20*, 205 (Aug. 2023). Publisher: Royal Society Publishing.
- [44] PARK, J., BAI, B., RYU, D., LIU, T., LEE, C., LUO, Y., LEE, M. J., HUANG, L., SHIN, J., ZHANG, Y., RYU, D., LI, Y., KIM, G., MIN, H.-s., OZCAN, A., AND PARK, Y. Artificial intelligence-enabled quantitative phase imaging methods for life sciences. *Nature Methods* (Oct. 2023).
- [45] ROBERT, D. Aerial electroreception. Current Biology 34, 20 (2024), R1018-R1023.
- [46] RONNEBERGER, O., FISCHER, P., AND BROX, T. U-net: Convolutional networks for biomedical image segmentation. In *Medical Image Computing and Computer-Assisted Intervention – MICCAI* 2015 (Cham, 2015), N. Navab, J. Hornegger, W. M. Wells, and A. F. Frangi, Eds., Springer International Publishing, pp. 234–241.
- [47] SINGH, S. P., WANG, L., GUPTA, S., GOLI, H., PADMANABHAN, P., AND GULYÁS, B. 3D Deep Learning on Medical Images: A Review. Sensors 20, 18 (Sept. 2020), 5097.
- [48] Sutton, G. P., Clarke, D., Morley, E. L., and Robert, D. Mechanosensory hairs in bumblebees (*Bombus terrestris*) detect weak electric fields. *PNAS 113*, 26 (2016), 7261–7265.
- [49] TREFETHEN, L. N. Numerical conformal mapping with rational functions. Comput. Methods Funct. Theory 20, 3 (2020), 369–387.
- [50] Turley, J., Chenchiah, I. V., Martin, P., Liverpool, T. B., and Weavers, H. Deep learning for rapid analysis of cell divisions in vivo during epithelial morphogenesis and repair. *eLife* 12 (Sept. 2024), RP87949.
- [51] Turley, J., Leong, K. W., and Chan, C. J. Novel imaging and biophysical approaches to study tissue hydraulics in mammalian folliculogenesis. *Biophysical Reviews* (Oct. 2024).
- [52] TURLEY, J., ROBERTSON, F., CHENCHIAH, I. V., LIVERPOOL, T. B., WEAVERS, H., AND MARTIN, P. Deep learning reveals a damage signalling hierarchy that coordinates different cell behaviours driving wound re-epithelialisation. *Development* 151, 18 (Sept. 2024), dev202943.
- [53] VILLARS, A., LETORT, G., VALON, L., AND LEVAYER, R. DeXtrusion: automatic recognition of epithelial cell extrusion through machine learning in vivo. *Development (Cambridge)* 150, 13 (July 2023). Publisher: Company of Biologists Ltd.
- [54] WOODBURN, F., O'REILLY, L., BENTALL, L., AND ROBERT, D. Electrostatic detection and electric signalling in plants: do flowers act as antennas? In *Journal of Physics: Conference Series* (2024), vol. 2702, IOP Publishing, p. 012012.
- [55] XUE, C., XU, L., WANG, H., LIU, H., YIN, J., LI, X., AND LI, B. A rational function approximation algorithm for the frequency sweep of microwave tube. In 2023 24th Int. Vacuum Electronics Conf. (IVEC) (2023), IEEE, pp. 1–2.